Yu *et al. Virology Journal* (2025) 22:159
https://doi.org/10.1186/s12985-025-02787-7

Virology Journal

RESEARCH Open Access

Evaluation of broad-spectrum protection by novel mRNA vaccines against SARS-CoV-2 variants (Delta, Omicron-BA.5, XBB-EG.5) in the golden hamster model

Tong Yu[1,2], JunHong Xing[1,3*], XinYu Zhuang[2*] and MingYao Tian[2*]

Abstract

Background The SARS-CoV-2 virus has continuously evolved, with new variants like Delta, Omicron-BA.5, and XBB-EG.5 posing challenges to vaccine efficacy. mRNA vaccines have emerged as a promising tool due to their rapid development and adaptability. This study evaluates the protective efficacy of six novel mRNA vaccine candidates against these variants using a golden hamster model.

Methods Six mRNA vaccines were designed, targeting the spike (S) and nucleocapsid (N) proteins of SARS-CoV-2. The vaccines were tested on golden hamsters, which were immunized and then challenged with Delta, Omicron-BA.5, and XBB-EG.5 variants. Key outcomes measured included body weight, viral RNA loads in various tissues, cytokine levels, and lung tissue pathology.

Results Hamsters vaccinated with the novel mRNA vaccines showed reduced weight loss, lower viral RNA loads in throat swabs and lung tissues, and reduced levels of pro-inflammatory cytokines compared to control groups. Additionally, vaccinated animals exhibited significantly less lung damage as evidenced by both histological and immunofluorescence analyses, especially in groups vaccinated with RBD-Fe, RE-N, and COVID-19 epitope formulations.

Conclusions These mRNA vaccines demonstrated broad protective efficacy against multiple SARS-CoV-2 variants. They elicited immune responses, reduced viral RNA loads, and mitigated inflammatory and pathological damage, highlighting their potential in combating rapidly evolving SARS-CoV-2 variants.

Keywords SARS-CoV-2, Delta, Omicron-BA.5, XBB-EG.5, mRNA vaccine

*Correspondence:
JunHong Xing
a18543127250@163.com
XinYu Zhuang
xinyuzhuang367@163.com
MingYao Tian
klwklw@126.com
[1]College of Veterinary Medicine, Jilin Agricultural University, Changchun, China
[2]Changchun Veterinary Research Institute, State Key Laboratory of Pathogen and Biosecurity, Key Laboratory of Jilin Province for Zoonosis Prevention and Control, Chinese Academy of Agricultural Sciences, Changchun, China
[3]College of Veterinary Medicine, Jilin Provincial Engineering Research Center of Animal Probiotics, Jilin Agricultural University, 2888 Xincheng Street, Changchun 130118, China

Introduction

SARS-CoV-2 (Severe Acute Respiratory Syndrome Coronavirus 2) is a single-stranded positive-sense RNA virus, classified within the Betacoronavirus genus of the Coronaviridae family [1]. Identified in 2019, it is associated with COVID-19 (Corona Virus Disease 2019), a novel respiratory illness known for its high transmissibility and severe symptoms such as fever, cough, difficulty breathing, and multi-organ failure [2, 3]. The virion of SARS-CoV-2 is spherical, approximately 100 nanometers in diameter, and is enveloped by a lipid bilayer membrane. This shell includes spike (S) proteins, nucleocapsid (N) proteins, membrane (M) proteins, and envelope (E) proteins, all of which play essential roles in viral assembly, replication, and immune evasion. The spike protein is particularly significant as it facilitates viral entry into host cells by binding to the ACE2 receptors on the surface of respiratory epithelial cells in humans and other mammals [4]. The genome of SARS-CoV-2 comprises about 30,000 nucleotides, encoding various non-structural proteins, such as RNA polymerase, and multiple key structural proteins. These proteins enable rapid viral replication within the host and provoke a robust immune response, leading to a spectrum of clinical manifestations [5]. Due to its high infectivity and propensity for mutation, SARS-CoV-2 continues to pose a substantial global public health threat. This has driven sustained international efforts among research institutions and companies to develop vaccines, explore therapeutic strategies, and establish effective control measures for long-term management of COVID-19 [6]. The deployment of severe acute respiratory syndrome coronavirus 2 (SARS-CoV-2) vaccines has significantly reduced morbidity and mortality worldwide [7]. However, the rapid evolution of SARS-CoV-2 continually threatens to compromise the effectiveness of these preventive and therapeutic options [1]. The mRNA vaccine, a critical innovation for public health against the COVID-19 pandemic, has demonstrated remarkable benefits [8]. It is noted for its rapid development, high customization potential, and scalable production. The mRNA vaccines operate based on fundamental biological principles, using synthetic mRNA molecules that encode viral proteins to stimulate the immune system to produce antibodies against these proteins. Upon vaccination, human cells read these mRNA instructions and produce viral surface antigens, such as the spike protein. These antigens are recognized as foreign substances by the body, triggering an immune response that includes the formation of memory B cells and T cells [9, 10]. Compared to traditional inactivated or attenuated vaccine platforms, mRNA vaccines offer significant advantages. Firstly, they do not contain live virus, thereby reducing the risk of infection. Secondly, mRNA can be rapidly produced and easily modified to respond to viral mutations. Additionally, because mRNA does not replicate within the body, its safety profile is relatively high. These benefits make mRNA technology an ideal choice for combating rapidly evolving viruses such as SARS-CoV-2 [11, 12]. In our study, we identified and selected the SARS-CoV-2 spike (S) and nucleocapsid (N) proteins as targets, due to their critical roles in viral interaction with host cells and their strong immunogenic properties. By precisely designing mRNA sequences to encode the functional and structural regions of these proteins, we ensured that the vaccine would elicit a robust antibody response [13, 14]. We employed chemical modifications to the mRNA to enhance its stability and translation efficiency, encapsulating it in lipid nanoparticles (LNPs). These nanocarriers improve the delivery of mRNA to immune cells, increasing vaccine efficacy, while also slowing the degradation of mRNA within the body, ensuring a sustained and long-lasting immune response [15–17].

The core mechanism of mRNA vaccines lies in their ability to stimulate both humoral and cellular immunity to provide lasting protection post-vaccination [18]. Humoral immunity involves the production of specific IgG antibodies against the SARS-CoV-2 spike protein, which can prevent the virus from binding to host cells. Cellular immunity, on the other hand, involves T cell responses, particularly $CD4^+$ and $CD8^+$ T cells, which can directly attack virus-infected cells or assist B cells in antibody production [19]. Preclinical studies and early clinical trials have extensively explored the immunogenicity of mRNA vaccines. These studies confirmed that mRNA vaccines induce a strong and lasting anti-spike protein response, demonstrating significant protective effects in mouse models. Large-scale, multicenter clinical trials, such as COVACTA and COMERCA, along with Phase III results from companies like Pfizer-BioNTech and Moderna, have shown that mRNA vaccines are equally effective in humans [20]. Real-world data further corroborates the efficacy of mRNA vaccines. This evidence includes not only the prevention of infection post-vaccination but also a significant reduction in hospitalization and mortality rates due to SARS-CoV-2. For instance, within months of vaccination, the risk of hospitalization among vaccinated individuals was reduced by approximately 50% compared to unvaccinated individuals, with a marked advantage in preventing severe cases and deaths [21, 22]. In conclusion, mRNA vaccines provide a robust tool for controlling the COVID-19 pandemic by inducing comprehensive immune responses. Their efficacy in both preclinical and real-world applications lays a solid foundation for global public health strategies.

SARS-CoV-2 variants spread rapidly and exhibit significant immune evasion. Currently, these variants coexist with humans, posing an ongoing threat to public health. Most vaccines administered are based on the

original wild-type strains, which are less effective against emerging variants. Therefore, the development of a safe and effective SARS-CoV-2 vaccine that provides broad-spectrum protection against these variants is of paramount importance for safeguarding public health. In this study, we designed and developed six novel SARS-CoV-2 mRNA candidate vaccines targeting the spike (S) and nucleocapsid (N) proteins. These vaccines included RBD-Fe, RBD, 2RBD, and ubiquitinated WT-N, RE-N, and COVID-19 epitopes. The vaccines were expressed in a eukaryotic expression system and combined with the lipid nanoparticle material SM102 to facilitate delivery. The immune protection mediated by both humoral and cellular immune responses was systematically analyzed. In addition, the vaccine was tested against four different SARS-CoV-2 strains: wild-type (WT), Delta, Omicron-BA.5, and XBB-EG.5 variants, and the protective efficacy was evaluated using the golden hamster model. The aim of this study was to develop a new SARS-CoV-2 mRNA vaccine with broad cross-protection against emerging variants, providing a strong defense against the ongoing evolution and mutation of the virus, and offering significant potential for controlling the spread of the pandemic and safeguarding public health.

Materials and methods

Cells, golden hamsters, and virus

293T cells were cultured in DMEM supplemented with 10% fetal bovine serum (FBS) at 37 °C. The SARS-CoV-2 Delta strain (CSTR.16698.06. NPRC6. CCPM-B-V-049-2105-6) was provided by Zhengfeng Qin. The SARS-CoV-2 Omicron-BA.5 strain (SARS-CoV-2 strain Omicron CoV/human/CHN_CVRI-12/2022) and SARS-CoV-2 XBB-EG.5 strain (SARS-CoV-2 strain EG.5.1.1 CoV/human/CHN_CVRI-06/2023) were isolated from patients. Specific pathogen-free male golden hamsters were obtained from Jilin Jintai Medicine Technology Co., Ltd. All animal studies were conducted in an Animal Biosafety Level 3 (ABSL-3) facility.

Design and Preparation of mRNA vaccines

Based on previous studies, RBD-Fe, RBD, 2RBD, WT-N, RE-N, and COVID-19 epitope mRNA vaccines were developed using a microfluidic device by optimizing mRNA sequence design, selecting appropriate nucleotide modifications, and improving lipid nanoparticle (LNP) formulations [17]. The mRNA sequences were designed to encode key SARS-CoV-2 proteins (spike and nucleocapsid proteins), with the nucleocapsid protein modified by ubiquitination. Specifically, the isopeptidase site residue G76 was replaced with non-cleavable valine residues (UbVR and UbVV) to enhance mRNA stability and translational efficiency [23]. Additionally, the vaccine formulation ensures long-term storage stability, immunogenicity, and durability. Briefly, the T7-FlashScribe Transcription Kit (CELLSCRIPT, Madison, WI, USA) was used to transcribe linearized pGEM-3Zf-n3 plasmids encoding luciferase (Luc), RBD-Fe, RBD monomer, RBD dimer (2RBD), ubiquitin-induced wild-type N protein (WT-N), recombinant N protein (Re-N), and COVID-19 epitopes using T7 RNA polymerase. The mRNA was capped with the ScriptCap™ Cap 1 Capping System (CELLSCRIPT, WI, USA) and purified using the MEGAclear Transcription Clean-Up Kit (ThermoFisher Scientific, Waltham, MA, USA). Purified mRNA was stored at -80 °C until further use. The mRNA was encapsulated in lipid nanoparticles (LNPs) with the composition SM-102: DSPC: CHO-HP: DSPE-MPEG2000 (mol: mol = 50: 10: 38.5: 1.5, N: P = 5.67: 1) using a microfluidic device to rapidly mix the mRNA aqueous solution and lipid solution, with a syringe pump infusing ethanol and aqueous phases at a 3:1 ratio. Concentration was performed using a 10kD ultrafiltration device (Millipore, Billerica, MA, USA). DOTAP and DOPE were purchased from Shanghai Aviva Pharmaceuticals, and DSPE-MPEG2000 was purchased from Xi'an Rui Xi Biotechnology Co., Ltd.

Animal immunization protocol

Four-week-old male golden hamsters were randomly divided into nine groups, with five hamsters per group, including six immunization groups (LNP/RBD-Fe, LNP/RBD, LNP/2RBD, LNP/WT-N, LNP/RE-N, and LNP/COVID-19 epitopes) and three control groups (LNP/Luc, LNP alone, and PBS alone). There were 9 groups in each batch, with a total of 3 batches of 135 mice. Each batch was challenged with SARS-CoV-2 Delta, SARS-CoV-2 Omicron-BA.5 and SARS-CoV-2 XBB-EG.5. The vaccines were administered intramuscularly on days 0, 14, and 28, with the immunization groups receiving 12 μg mRNA. Control groups received 12 μg LNP or PBS. Forty-two days post-initial immunization, each hamster was anesthetized by isoflurane inhalation and challenged with 1×10^5 $TCID_{50}$ SARS-CoV-2 virus via nasal drops. Weight and survival were monitored on days 1, 3, and 5 post-challenge. Throat swabs were collected on days 3 and 5 post-infection for viral load detection (N and E genes). On day 5 post-infection, lung, nasal turbinate, and trachea samples were collected for viral load assessment (N and E genes), inflammatory cytokine transcription levels (IL-1β, IL-6, MCP-1, TNF-α, CCL3, CCL5), and protein expression levels (IL-1β, IL-2, IL-6, IL-10, IFN-γ, TNF-α). Remaining lung tissue was used for pathological and immunofluorescence analyses. All experimental procedures (including vaccine administration and viral infection) were conducted under anesthesia to ensure the animals' comfort and to avoid stress responses. Isoflurane was used as the anesthetic agent, with a concentration of 5% for induction and 2–3% for maintenance,

administered via a sealed anesthesia box. At the end of the experiments, the hamsters were euthanized under anesthesia. During euthanasia, Isoflurane was also used, with a concentration of 5% for deep anesthesia, followed by cervical dislocation while in a deep anesthetic state. All procedures conformed to the guidelines set by the Animal Ethics Committee.

ELISA

Cytokines IL-1β, IL-2, IL-6, IL-10, IFN-γ, and TNF-α in hamster lung homogenates were measured using ELISA kits from Shanghai Hengyuan Biotechnology Co., Ltd., according to the manufacturer's instructions.

RNA extraction

RNA was extracted from hamster throat swabs, lung, nasal turbinate, and trachea using the TotalRNAExtractor kit. Tissue samples were homogenized with TotalRNAExtractor, and throat swabs were mixed with TotalRNAExtractor and incubated at room temperature for 5–10 min. Chloroform was added, and samples were centrifuged at 4 °C. The aqueous phase was collected, mixed with anhydrous ethanol, and loaded onto an adsorption column, followed by centrifugation and washing with RPE Solution. RNA was eluted with DEPC-treated water and stored at -80 °C.

Table 1 The primer sequences for qPCR

Primers	Sequence (5′ → 3′)
IL-6-F	TGTCTTCTTGGGACTGCTGC
IL-6-R	CCAAACCTCCGACTTGTTGA
TNF-α-F	AGAATCCGGGCAGGTCTACT
TNF-α-R	TATCCCGGCAGCTTGTGTTT
MCP-1-F	TCCTGCAAGTCAATCCTGCC
MCP-1-R	GAAGTGATGGAGAGACGGGC
IL-1β-F	TGAGGTTGACGGGCTCCAAAA
IL-1β-R	ACAGGGGTGTTCCACAGCTT
CCL-3-F	GGTCCAAGAGTACGTCGCTG
CCL-3-R	GAGTTGTGGAGGTGGCAAGG
CCL-5-F	ACTGCCTCGTGTTCACATCA
CCL-5-R	TTCGGGTGACAAAAACGACT
GAPDH-F	AACTTTGGCATTGTGGAAG
GAPDH-R	CGACATGTGAGATCCACGAC
β-actin-F	CCATTGGCAACGAGCGGTT
β-actin-R	CCACAGGATTCCATACCCAGGAAG
COVID-19 N-F	GGGGAACTTCTCCTGCTAGAAT
COVID-19 N-R	CAGACATTTTGCTCTCAAGCTG
COVID-19 N-P	TTGCTGCTGCTTGACAGATT
COVID-19 sgE-F	CGATCTCTTGTAGATCTGTTCTC
COVID-19 sgE-R	ATATTGCATTGCAGCAGTACGCACA
COVID-19 sgE-P	ACACTAGCCATCCTTACTGCGCTTCG

qPCR

RNA extracted from hamster throat swabs, lung, nasal turbinate, and trachea was subjected to qPCR using the UNlQ-10 Column Trizol Total RNA Isolation Kit (Sangon Biotech, Shanghai). HiScript II U + One Step qRT-PCR Probe Kit and HiScript II One Step qRT-PCR SYBR Green Kit (Vazyme, China) were used for qPCR, with probes and primers synthesized by Jilin Kumei Biotechnology Co., Ltd. Specific probes and primers were shown in Table 1.

Pathological analysis

Hamster lung tissues were fixed in 10% neutral-buffered formalin for 24 h, dehydrated, embedded in paraffin, and sectioned at 4 μm thickness. Sections were stained with hematoxylin and eosin (H&E) and examined under a light microscope to evaluate tissue structure and inflammation.

Immunofluorescence

Lung tissues were fixed in 4% paraformaldehyde for 4 h, dehydrated overnight, embedded in OCT, and sectioned at 5 μm thickness. Sections were washed with PBS, permeabilized with 0.1% Triton X-100, and blocked with 10% goat serum. They were then incubated with primary antibody against SARS-CoV-2 spike protein (Sinobiological, 40589-T62) and fluorescent secondary antibody, followed by DAPI nuclear staining. Fluorescence microscopy was used to observe and quantify spike protein expression.

Statistical analysis

All data are presented as mean ± standard deviation (SD). Statistical analyses were performed using one-way ANOVA with GraphPad Prism 10.2.1. P-values are indicated as follows: $^{*}P < 0.05$, $^{**}P < 0.01$, $^{***}P < 0.001$, $^{****}P < 0.0001$.

Results

Evaluation of protective efficacy against SARS-CoV-2 Delta variant

In this study, we evaluated the protective efficacy of novel mRNA vaccines against the SARS-CoV-2 Delta variant in the golden hamster model. Results indicated that hamsters vaccinated with RBD-Fe, RBD, 2RBD, WT-N, RE-N, and COVID-19 epitope vaccines maintained more stable body weights post-infection (Fig. 1A), whereas the control groups (Luc, LNP, and PBS) experienced significant weight loss, suggesting that vaccination helped prevent the infection-associated weight loss. Viral RNA load analysis revealed that vaccinated hamsters had significantly lower viral RNA loads in throat swabs on days 3 and 5 post-infection compared to controls (Fig. 1B and C). Notably, the RBD-Fe, RBD, 2RBD, WT-N, RE-N and COVID-19 epitope groups exhibited significantly lower

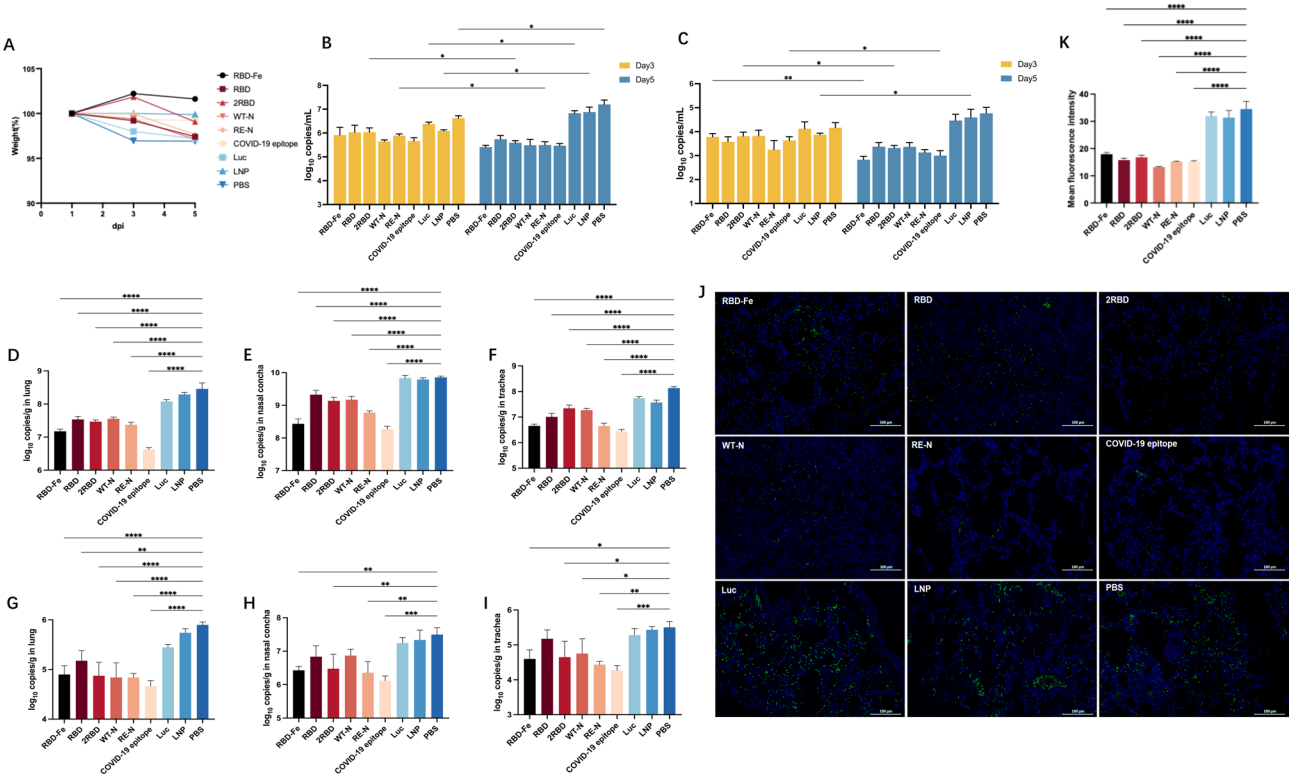

Fig. 1 Protective effects of novel mRNA vaccines against the SARS-CoV-2 Delta strain. (**A**) Weight change rate in golden hamsters infected with the SARS-CoV-2 Delta strain. Viral load analysis in hamsters post-infection with SARS-CoV-2 N and E genes: (**B**) Throat swab N, (**C**) Throat swab E, (**D**) Lung N, (**G**) Lung E, (**E**) Nasal turbinate N, (**H**) Nasal turbinate E, (**F**) Trachea N, (**I**) Trachea E. (**J**) Immunofluorescence analysis of SARS-CoV-2 S protein in hamster lung tissues. (**K**) Quantitative analysis of spike protein fluorescence intensity in the lung, showing the mean fluorescence intensity. **P*<0.05, ***P*<0.01, ****P*<0.001, *****P* < 0.0001

viral RNA loads, indicating effective suppression of viral replication. Viral RNA load assessments in the lungs, nasal turbinates, and trachea showed that vaccinated groups had significantly lower viral RNA loads compared to controls (Figs. 1D-I). In particular, the lungs of the RBD-Fe, RBD, 2RBD, WT-N, RE-N and COVID-19 epitope groups showed markedly reduced viral RNA loads, demonstrating significant inhibition of viral replication. Similar trends were observed in nasal turbinates and trachea, with vaccinated groups showing significantly lower viral RNA loads than controls. Immunofluorescence analysis further validated these results. Vaccinated hamsters displayed fewer SARS-CoV-2 S protein antigen signals in lung tissues (Fig. 1J and K), especially in the 2RBD, RE-N and COVID-19 epitope groups, indicating effective inhibition of the virus in the lungs.

Inflammatory response and pathological damage induced by SARS-CoV-2 Delta variant

We also assessed the impact of novel mRNA vaccines on the inflammatory response and pathological damage caused by the SARS-CoV-2 Delta variant in the golden hamster model. Results showed that vaccinated hamsters had significantly lower expression levels of inflammatory cytokines in lung tissues post-infection compared to controls (Luc, LNP, and PBS). qPCR analysis indicated that vaccinated hamsters had significantly reduced gene expression of inflammatory cytokines IL-1β, TNF-α, IL-6, MCP-1, CCL3, and CCL5 in lung tissues post-infection (Figs. 2A-F). Particularly, the RBD-Fe, 2RBD, RE-N and COVID-19 epitope groups exhibited significantly lower expression levels of these cytokines, indicating effective mitigation of lung inflammation. ELISA analysis confirmed these findings, showing significantly lower protein levels of IL-1β, IL-6, IFN-γ, and TNF-α in the lung tissues of vaccinated hamsters (Figs. 2H-M). Notably, IL-6 and TNF-α, key pro-inflammatory cytokines, were significantly reduced in the RBD-Fe, RBD, 2RBD, RE-N and COVID-19 epitope groups, while expression levels of anti-inflammatory cytokine IL-10 and regulatory cytokine IL-2 were significantly increased, demonstrating the potential of these vaccines to reduce inflammatory responses. H&E staining and pathological scoring analysis showed that pathological damage in the lung tissue of vaccinated hamsters was significantly alleviated (Fig. 2G and N). Compared to the control group, the vaccinated group exhibited more intact lung tissue structure, reduced inflammatory cell infiltration, less tissue damage,

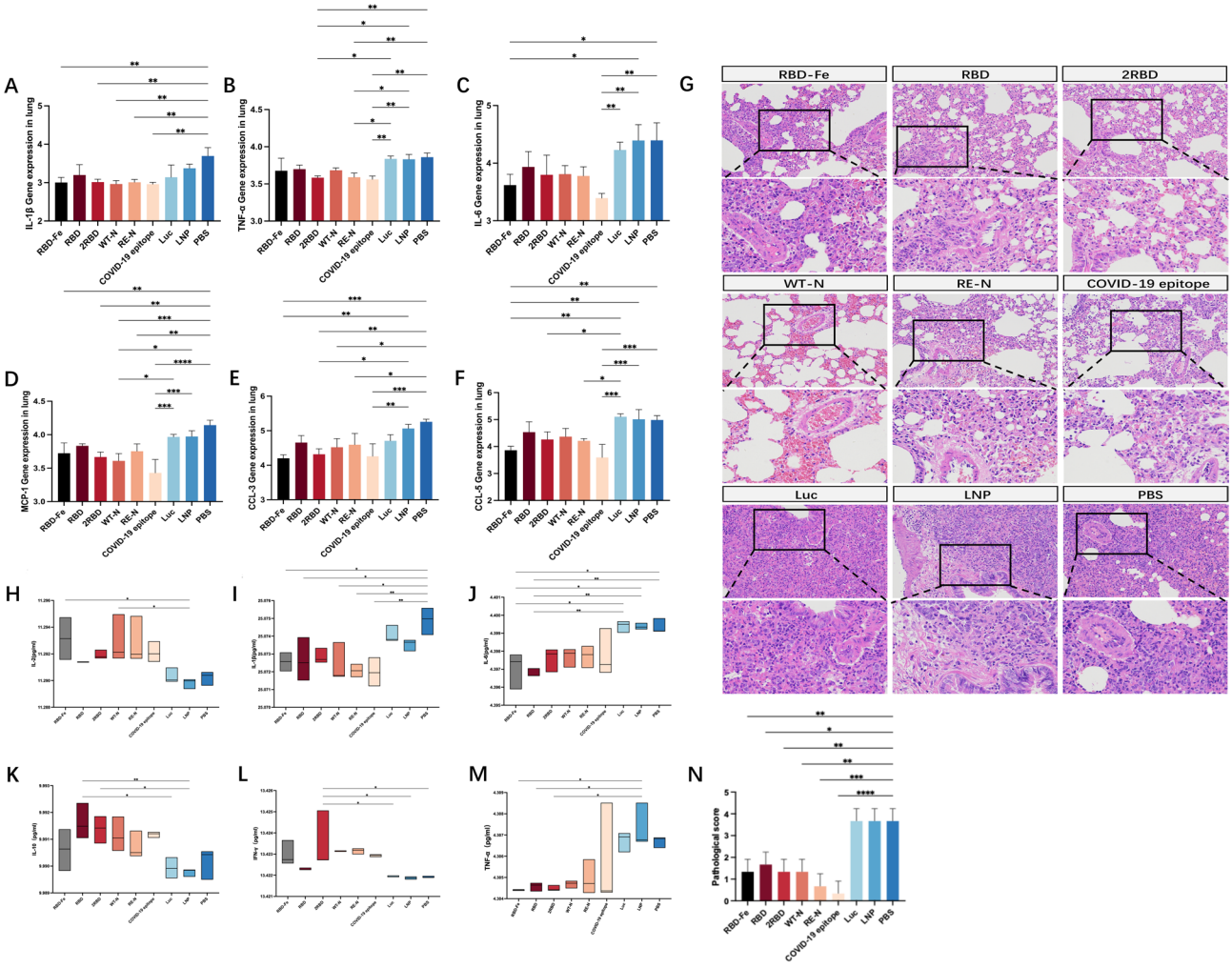

Fig. 2 Inflammatory response and pathological damage analysis of novel mRNA vaccines against the SARS-CoV-2 Delta strain. qPCR analysis of relative expression of inflammatory cytokines in lung tissues of hamsters infected with the SARS-CoV-2 Delta strain: (**A**) IL-1β, (**B**) TNF-α, (**C**) IL-6, (**D**) MCP-1, (**E**) CCL-3, (**F**) CCL-5. ELISA analysis of cytokine expression in hamster lung tissues: (**H**) IL-2, (**I**) IL-1β, (**J**) IL-6, (**K**) IL-10, (**L**) IFN-γ, (**M**) TNF-α. (**G**) Pathological damage analysis of hamster lungs (H&E staining). (**N**) Blinded sections were evaluated to determine pathological severity. To assess overall histological changes, lung tissue sections were scored according to criteria specified by the expert panel. The scoring system used was as follows: 0, no pathological changes; 1, affected area (≤ 20%); 2, affected area (≤ 50%, > 20%); 3, affected area (> 50%, ≤ 80%); 4, affected area (> 80%). **P*<0.05, ***P*<0.01, ****P*<0.001, *****P* < 0.0001

decreased perivascular edema, mild thickening of the alveolar walls, and reduced vascular congestion in the interstitium. In contrast, the control group showed evident pathological damage, including extensive inflammatory cell infiltration and disruption of tissue architecture. Particularly, the RBD-Fe, RE-N and COVID-19 epitope groups maintained better structural integrity in lung tissues, indicating significant protective effects.

Evaluation of protective efficacy against SARS-CoV-2 Omicron-BA.5 variant

We evaluated the protective efficacy of novel mRNA vaccines against the SARS-CoV-2 Omicron-BA.5 variant in the golden hamster model. Results indicated that vaccinated hamsters experienced less weight change post-infection compared to control groups (Luc, LNP, and PBS), which showed significant weight loss (Fig. 3A). This finding suggests that vaccination with these vaccines effectively reduces weight loss associated with infection by the Omicron-BA.5 variant. Viral RNA load analysis revealed significantly lower viral RNA loads in throat swabs of vaccinated groups on days 3 and 5 post-infection compared to controls (Fig. 3B and C), with RBD-Fe, RE-N and COVID-19 epitope groups showing significant viral suppression. Further tissue viral RNA load analysis indicated that vaccinated hamsters had significantly lower viral RNA loads in the lungs (Fig. 3D and G), nasal turbinates (Figs. 3E and H), and trachea (Fig. 3F and I) compared to controls, particularly in the RBD-Fe, 2RBD, RE-N and COVID-19 epitope groups, demonstrating effective viral inhibition in multiple respiratory tissues. Immunofluorescence analysis showed a significant

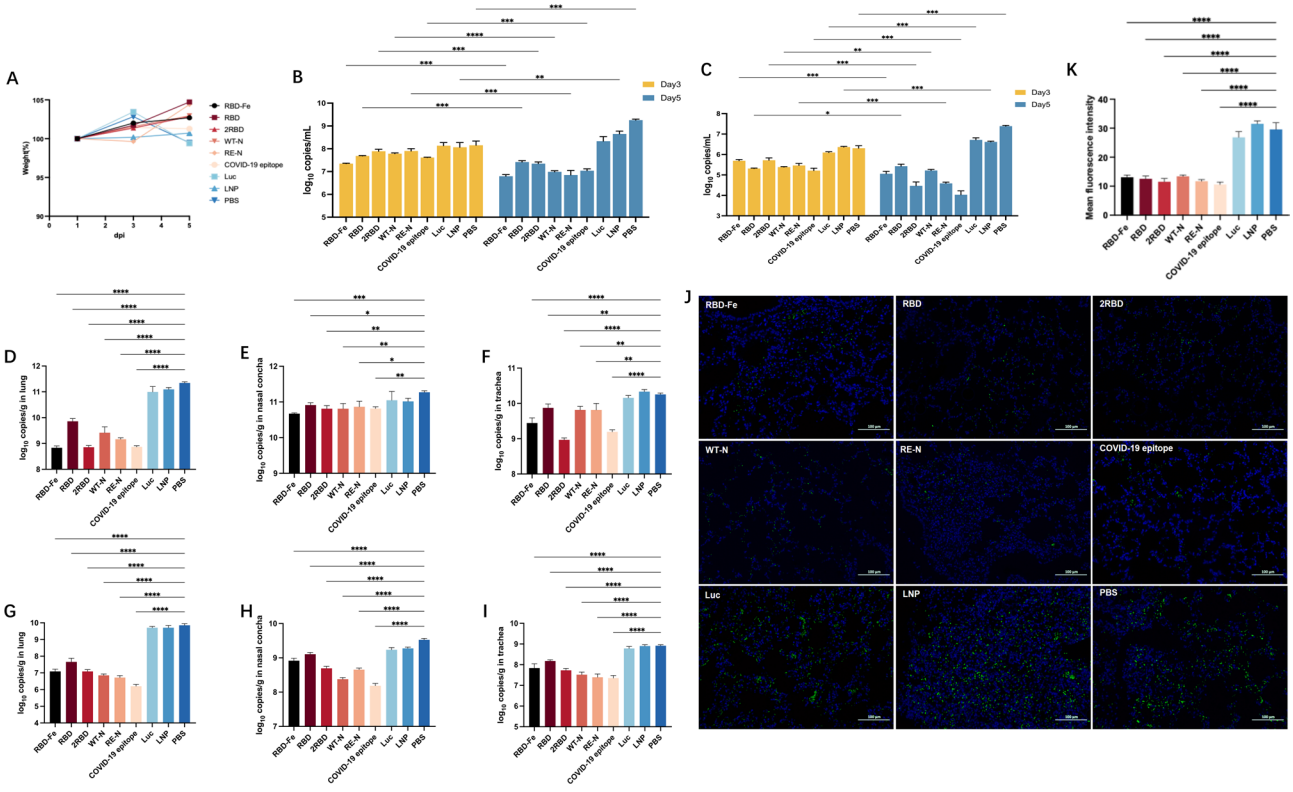

Fig. 3 Protective effects of novel mRNA vaccines against the SARS-CoV-2 Omicron-BA.5 strain. (**A**) Weight change rate in golden hamsters infected with the SARS-CoV-2 Omicron-BA.5 strain. Viral load analysis in hamsters post-infection with SARS-CoV-2 N and E genes: (**B**) Throat swab N, (**C**) Throat swab E, (**D**) Lung N, (**G**) Lung E, (**E**) Nasal turbinate N, (**H**) Nasal turbinate E, (**F**) Trachea N, (**I**) Trachea E. (**J**) Immunofluorescence analysis of SARS-CoV-2 S protein in hamster lung tissues. (**K**) Quantitative analysis of spike protein fluorescence intensity in the lung, showing the mean fluorescence intensity. **P*<0.05, ***P*<0.01, ****P*<0.001, *****P* < 0.0001

reduction in SARS-CoV-2 S protein presence in the lung tissues of vaccinated hamsters (Fig. 3J and K). The 2RBD, RE-N and COVID-19 epitope groups exhibited a notable decrease in viral antigens in lung tissues, further confirming the protective effects of these vaccines.

Inflammatory response and pathological damage induced by SARS-CoV-2 Omicron-BA.5 variant

Additionally, we assessed the impact of novel mRNA vaccines on the inflammatory response and pathological damage caused by the SARS-CoV-2 Omicron-BA.5 variant in the golden hamster model. Results showed significantly lower expression levels of inflammatory cytokines in lung tissues of vaccinated hamsters post-infection compared to controls (Luc, LNP, and PBS). qPCR analysis indicated that vaccinated groups had significantly reduced gene expression of inflammatory cytokines IL-1β (Fig. 4A), TNF-α (Fig. 4B), IL-6 (Fig. 4C), MCP-1 (Fig. 4D), CCL3 (Fig. 4E), and CCL5 (Fig. 4F) in lung tissues post-infection. Particularly, the RBD-Fe, 2RBD, RE-N and COVID-19 epitope groups exhibited significantly lower expression levels of these cytokines, indicating effective reduction of lung inflammation. ELISA analysis confirmed these findings, showing significantly lower protein levels of IL-1β (Fig. 4I), IL-6 (Fig. 4J), IFN-γ (Fig. 4L), and TNF-α (Fig. 4M) in lung tissues of vaccinated hamsters. The expression of regulatory cytokines IL-2 (Fig. 4H) and IL-10 (Fig. 4K) was significantly increased in vaccinated groups, demonstrating the potential of these vaccines to reduce inflammatory responses. H&E staining and pathological scoring analysis showed significantly less pathological damage in the lung tissues of vaccinated hamsters (Fig. 4G and N). Compared to the control group, the vaccinated group exhibited more intact lung tissue structure, reduced inflammatory cell infiltration, less tissue damage, mild thickening of the alveolar walls, decreased alveolar expansion, reduced hemorrhage in the bronchioles, and less epithelioid cell proliferation. In contrast, the control group showed pronounced pathological damage, including extensive inflammatory cell infiltration and disruption of tissue architecture.

Evaluation of protective efficacy against SARS-CoV-2 XBB-EG.5 variant

We also evaluated the protective efficacy of novel mRNA vaccines against the SARS-CoV-2 XBB-EG.5 variant in the golden hamster model. Results indicated that

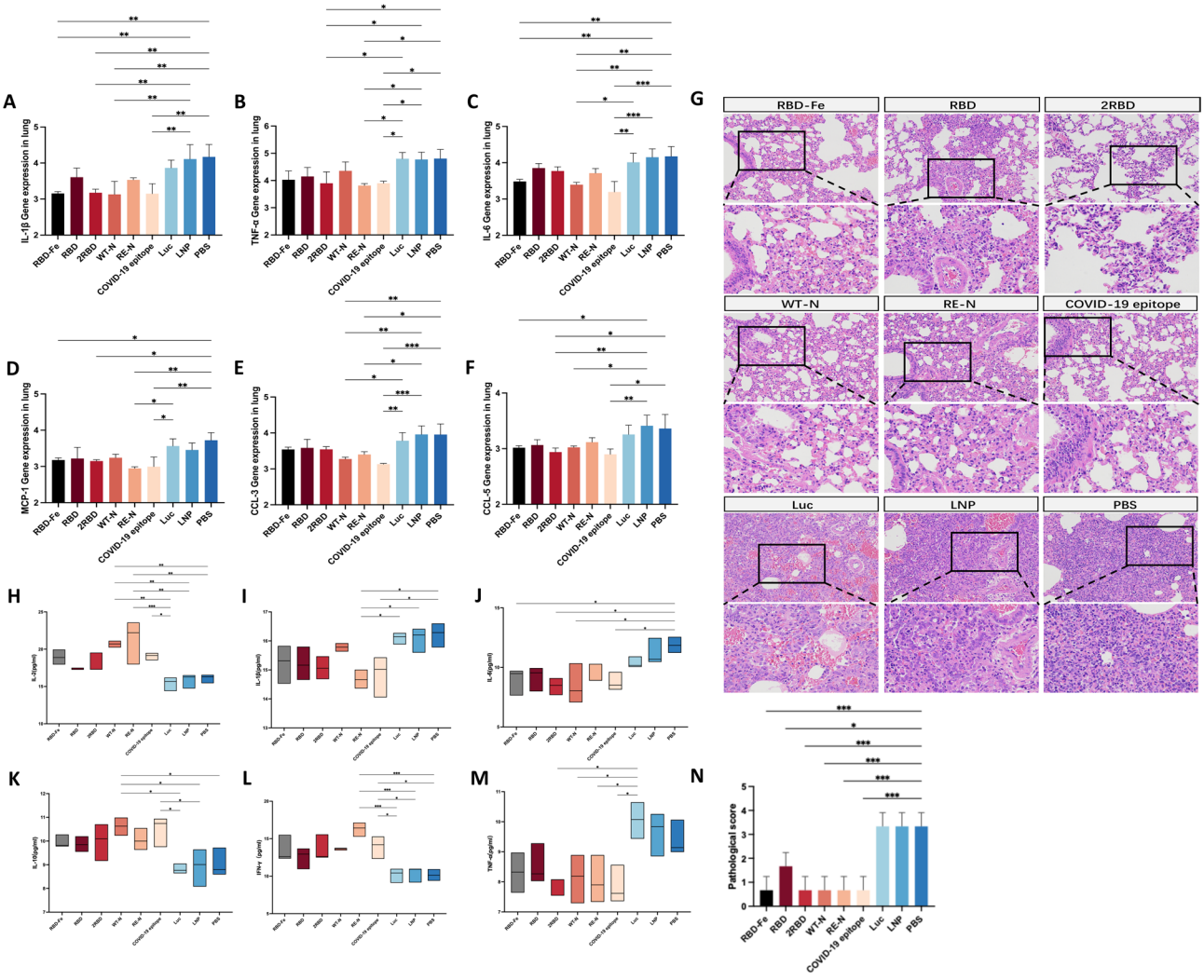

Fig. 4 Inflammatory response and pathological damage analysis of novel mRNA vaccines against the SARS-CoV-2 Omicron-BA.5 strain. qPCR analysis of relative expression of inflammatory cytokines in lung tissues of hamsters infected with the SARS-CoV-2 Omicron-BA.5 strain: (**A**) IL-1β, (**B**) TNF-α, (**C**) IL-6, (**D**) MCP-1, (**E**) CCL-3, (**F**) CCL-5. ELISA analysis of cytokine expression in hamster lung tissues: (**H**) IL-2, (**I**) IL-1β, (**J**) IL-6, (**K**) IL-10, (**L**) IFN-γ, (**M**) TNF-α. (**G**) Pathological damage analysis of hamster lungs (H&E staining). (**N**) Blinded sections were evaluated to determine pathological severity. To assess overall histological changes, lung tissue sections were scored according to criteria specified by the expert panel. The scoring system used was as follows: 0, no pathological changes; 1, affected area (≤ 20%); 2, affected area (≤ 50%, > 20%); 3, affected area (> 50%, ≤ 80%); 4, affected area (> 80%). **P*<0.05, ***P*<0.01, ****P*<0.001

vaccinated hamsters maintained stable body weights post-infection compared to control groups (Luc, LNP, and PBS), which showed significant weight loss (Fig. 5A). This finding suggests that vaccination with these vaccines effectively reduces weight loss associated with infection by the XBB-EG.5 variant. Viral RNA load analysis revealed significantly lower viral RNA loads in throat swabs of vaccinated hamsters on days 3 and 5 post-infection compared to controls (Fig. 5B and C), with 2RBD and COVID-19 epitope groups exhibiting strong viral suppression. Further tissue viral RNA load analysis indicated that vaccinated hamsters had significantly lower viral RNA loads in the lungs (Fig. 5D and G), nasal turbinates (Fig. 5E and H), and trachea (Fig. 5F and I) compared to controls, demonstrating effective viral inhibition in multiple respiratory tissues. Immunofluorescence analysis showed a significant reduction in SARS-CoV-2 S protein presence in the lung tissues of vaccinated hamsters (Fig. 5J and K), particularly in the 2RBD, WT-N, RE-N and COVID-19 epitope groups, further confirming the protective effects of these vaccines.

Inflammatory response and pathological damage induced by SARS-CoV-2 XBB-EG.5 variant

We also assessed the impact of novel mRNA vaccines on the inflammatory response and pathological damage caused by the SARS-CoV-2 XBB-EG.5 variant in the golden hamster model. Results showed significantly

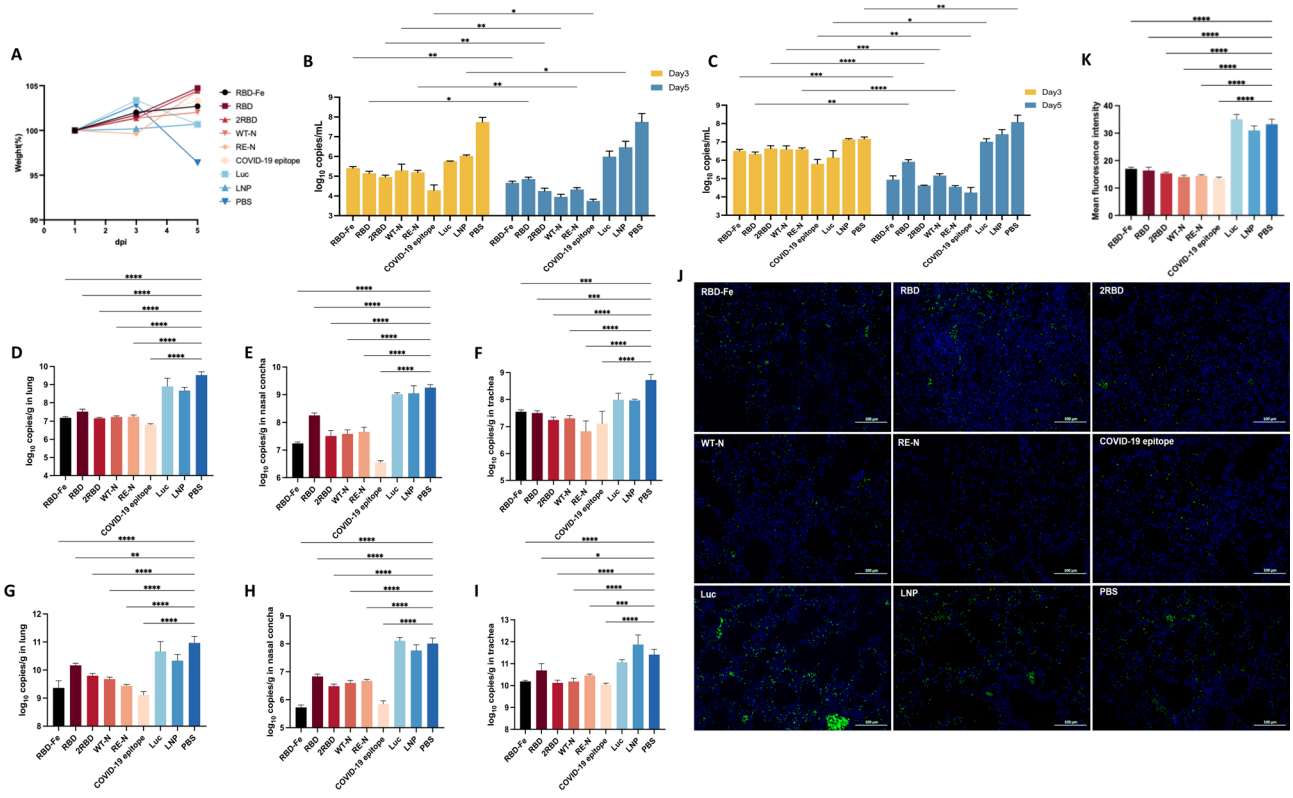

Fig. 5 Protective effects of novel mRNA vaccines against the SARS-CoV-2 XBB-EG.5 strain. (**A**) Weight change rate in golden hamsters infected with the SARS-CoV-2 XBB-EG.5 strain. Viral load analysis in hamsters post-infection with SARS-CoV-2 N and E genes: (**B**) Throat swab N, (**C**) Throat swab E, (**D**) Lung N, (**G**) Lung E, (**E**) Nasal turbinate N, (**H**) Nasal turbinate E, (**F**) Trachea N, (**I**) Trachea E. (**J**) Immunofluorescence analysis of SARS-CoV-2 S protein in hamster lung tissues. (**K**) Quantitative analysis of spike protein fluorescence intensity in the lung, showing the mean fluorescence intensity. **P*<0.05, ***P*<0.01, ****P*<0.001, ****P*<0.001, *****P* < 0.0001

lower expression levels of inflammatory cytokines in lung tissues of vaccinated hamsters post-infection compared to controls (Luc, LNP, and PBS). qPCR analysis indicated that vaccinated groups had significantly reduced gene expression of inflammatory cytokines IL-1β (Fig. 6A), TNF-α (Fig. 6B), IL-6 (Fig. 6C), MCP-1 (Fig. 6D), CCL3 (Fig. 6E), and CCL5 (Fig. 6F) in lung tissues post-infection. Particularly, the RBD-Fe, 2RBD, RE-N and COVID-19 epitope groups exhibited significantly lower expression levels of these cytokines, indicating effective reduction of lung inflammation. ELISA analysis showed significantly lower protein levels of IL-1β (Fig. 6I), IL-6 (Fig. 6J), IFN-γ (Fig. 6L), and TNF-α (Fig. 6M) in lung tissues of vaccinated hamsters. IL-2 (Fig. 6H) and IL-10 (Fig. 6K) expression levels were significantly increased in vaccinated groups, demonstrating the potential of these vaccines to reduce inflammatory responses. Additionally, H&E staining and pathological scoring analysis showed that vaccinated hamsters exhibited significantly reduced pathological damage in lung tissues (Fig. 6G and N). The lung tissue of the vaccinated group was more intact, with reduced inflammatory cell infiltration, less tissue damage, mild thickening of the alveolar walls, well-preserved alveolar structure, and reduced loosening of connective tissue. In contrast, the control group exhibited significant pathological damage in the lungs, including extensive parenchymal lesions and destruction of the alveolar architecture, which were caused by widespread inflammatory cell infiltration.

Discussion

This study evaluated the protective efficacy of several novel mRNA vaccines in a golden hamster model against SARS-CoV-2 variants, including Delta, Omicron-BA.5, and XBB-EG.5. The vaccines significantly mitigated infection-induced weight loss and reduced viral RNA loads in throat swabs, lungs, nasal turbinates, and trachea. Moreover, the vaccinated groups exhibited significant reductions in inflammatory responses and pathological damage, demonstrating the potential applicability of these mRNA vaccines in controlling COVID-19 and its variants (Fig. 7).

Effective vaccines are crucial for controlling the COVID-19 pandemic, especially as countries begin to ease non-pharmaceutical interventions like social distancing, travel restrictions, and quarantines. Since the outbreak, new SARS-CoV-2 variants have emerged, each with varying levels of virulence, transmissibility, and

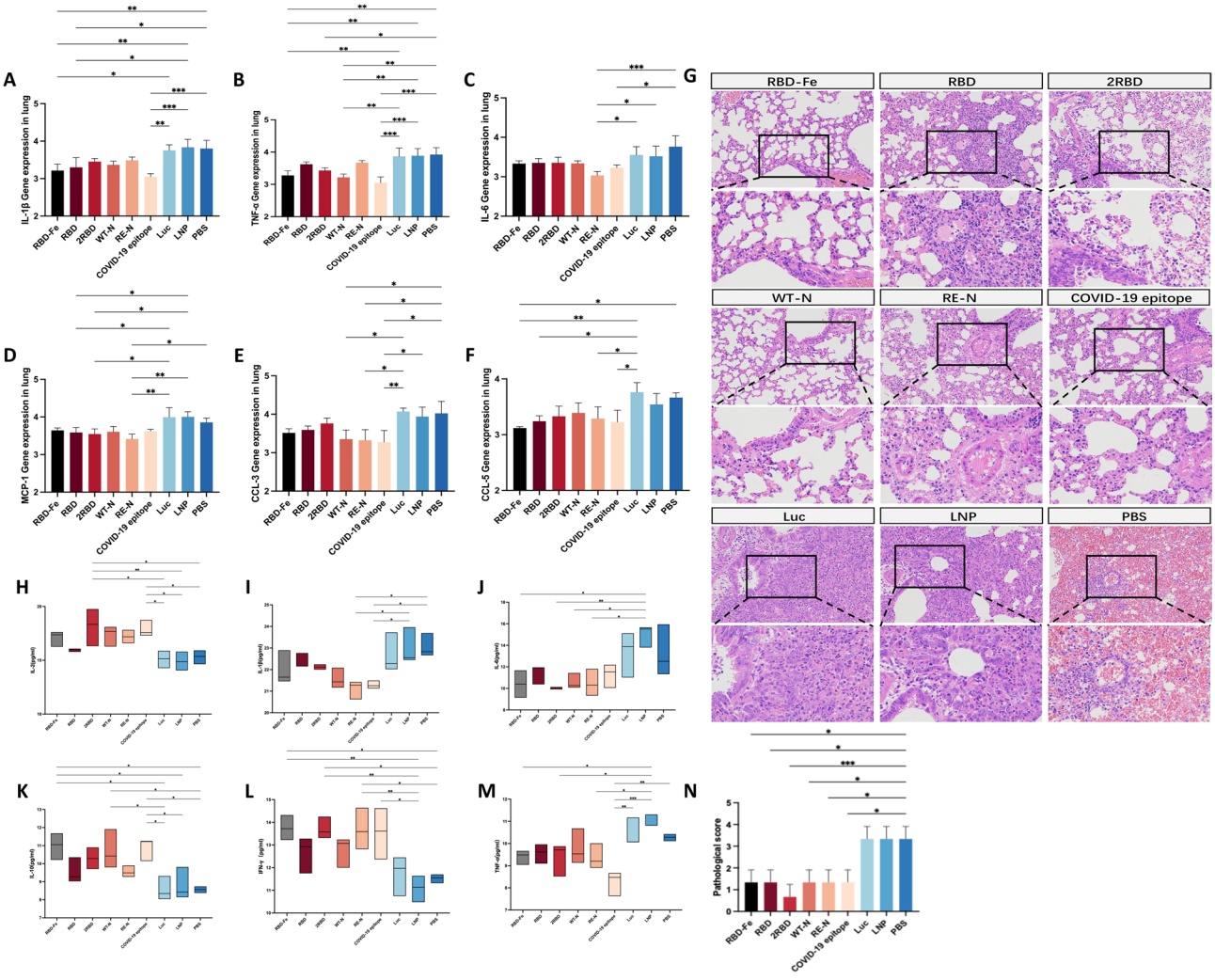

Fig. 6 Inflammatory response and pathological damage analysis of novel mRNA vaccines against the SARS-CoV-2 XBB-EG.5 strain. qPCR analysis of relative expression of inflammatory cytokines in lung tissues of hamsters infected with the SARS-CoV-2 XBB-EG.5 strain: (**A**) IL-1β, (**B**) TNF-α, (**C**) IL-6, (**D**) MCP-1, (**E**) CCL-3, (**F**) CCL-5. ELISA analysis of cytokine expression in hamster lung tissues: (**H**) IL-2, (**I**) IL-1β, (**J**) IL-6, (**K**) IL-10, (**L**) IFN-γ, (**M**) TNF-α. (**G**) Pathological damage analysis of hamster lungs (H&E staining). (**N**) Blinded sections were evaluated to determine pathological severity. To assess overall histological changes, lung tissue sections were scored according to criteria specified by the expert panel. The scoring system used was as follows: 0, no pathological changes; 1, affected area (≤ 20%); 2, affected area (≤ 50%, > 20%); 3, affected area (> 50%, ≤ 80%); 4, affected area (> 80%). **P*<0.05, ***P*<0.01, ****P*<0.001

immune evasion capabilities, affecting the efficacy of public health measures, diagnostics, vaccines, and treatments [24]. Animal models that mimic varying degrees of clinical disease manifestations can accelerate the development of treatments and vaccines for COVID-19 [25]. During the early stages of the COVID-19 pandemic, non-human primates, ferrets [26], and other animal models were used, leading to the conclusion that golden hamsters are a valuable model for evaluating SARS-CoV-2 and variant countermeasures [27]. Golden hamsters are easily infected with SARS-CoV-2 and exhibit pathological changes in lung tissues similar to those observed in COVID-19 patients [28]. Our previous studies have designed and validated SARS-CoV-2 2RBD and RBD-Fe mRNA vaccines, showing higher specific antibody levels. Even after serum dilution, these vaccines maintained higher specific IgG titers and enhanced the production of neutralizing antibodies [17]. The receptor-binding domain (RBD) of SARS-CoV-2, when conjugated to ferritin, can self-assemble into nanoparticle structures, significantly enhancing the immunogenicity of the vaccine. Previous studies have demonstrated that ferritin-bound RBD can greatly increase antigenicity through multivalent presentation, promoting stronger B cell responses and neutralizing antibody production [29]. In our study, animals vaccinated with the RBD-Fe vaccine exhibited significantly less weight loss post-infection and a marked reduction in viral RNA load compared to control groups. Moreover, the expression levels of inflammatory cytokines such as IL-1β, TNF-α, and IL-6 were significantly

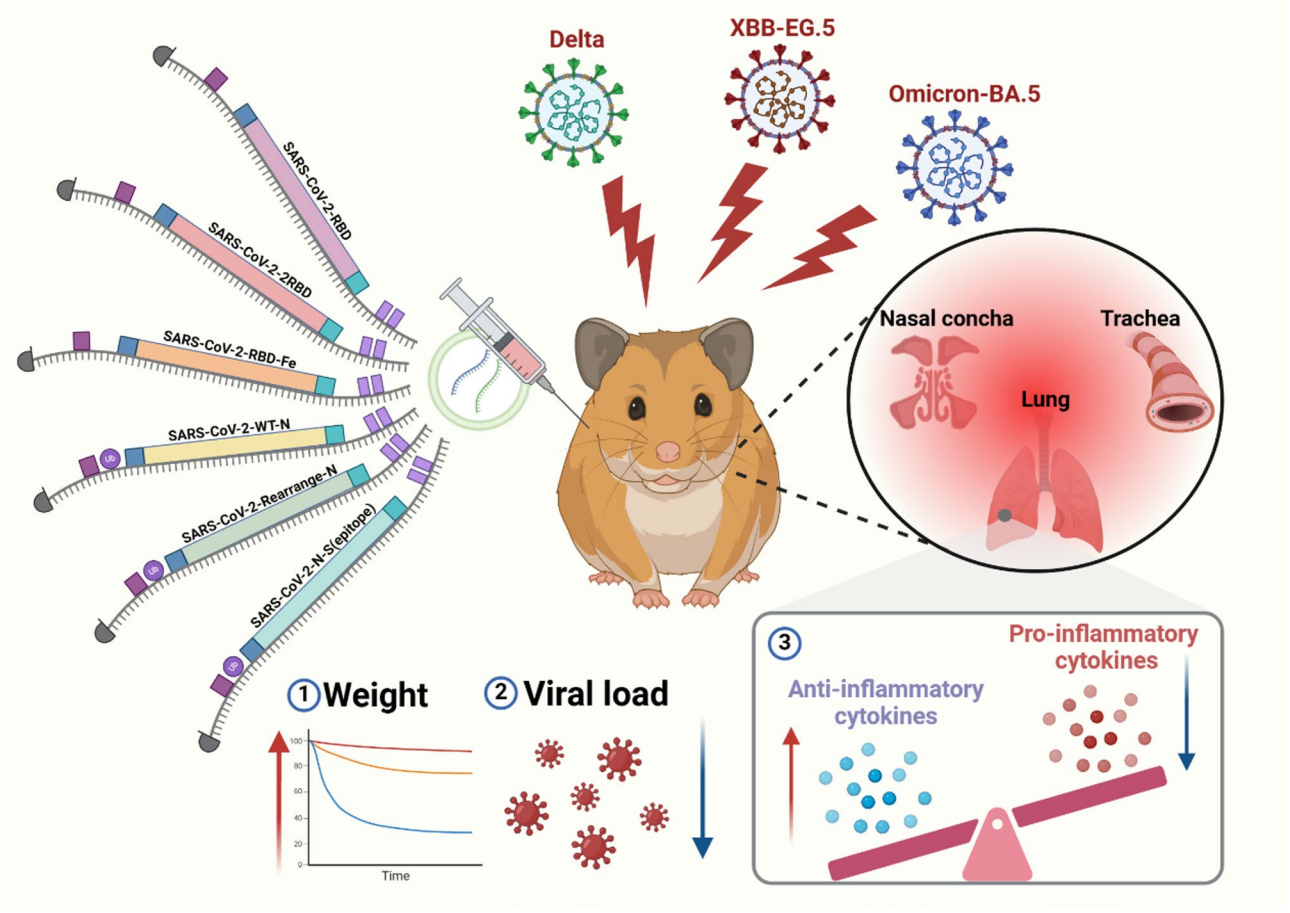

Fig. 7 Protective effects of novel mRNA vaccines against SARS-CoV-2 Delta, Omicron-BA.5, and XBB-EG.5 strains in golden hamsters

lower in the RBD-Fe vaccine group, indicating potent anti-inflammatory effects and tissue protection.

Neutralizing antibodies are one of the main immune effects against SARS-CoV-2. Studies have shown that specific antibodies can neutralize virus particles and prevent them from entering host cells. The S protein of SARS-CoV-2 is a key mediator for the virus to invade cells. Specific neutralizing antibodies bind to the S protein and prevent it from binding to the ACE2 receptor, thereby effectively preventing the virus from invading and infecting [30]. Given the high mutation rate of SARS-CoV-2, relying solely on neutralizing antibodies may not provide adequate protection. In addition to humoral immunity, cell-mediated immunity is strongly induced by the SARS-CoV-2 vaccines and infections. It has been shown that T-cell responses elicited by both infections and vaccinations are long-lasting and cross-reactive between virus variants [31–33], emphasizing the importance of cell-mediated immunity in the protection against a severe disease [34]. We designed a SARS-CoV-2 vaccine that elicits a specific cytotoxic T lymphocyte (CTL) response rather than a specific antibody response to prevent SARS-CoV-2 invasion [35, 36]. Cellular immune responses typically target conserved regions of the virus, which are relatively stable and less prone to mutations. While some viruses may evade neutralizing antibody recognition through escape mutations, cellular immune responses are generally harder for viruses to evade. Thus, vaccines based on cellular immunity can better adapt to viral mutations, providing durable protection and reducing susceptibility to variants, effectively combating viral escape mutations [37]. In summary, our study highlights the effectiveness of novel mRNA vaccines in inducing both humoral and cellular immune responses, reducing viral RNA loads, and mitigating inflammatory and pathological damage in the golden hamster model. These findings underscore the potential of mRNA vaccines in addressing the ongoing challenges posed by SARS-CoV-2 variants and contribute to the broader development of vaccines for other infectious diseases.

Traditionally, neutralizing antibodies and CTL responses are crucial for preventing viral infections [38]. This study focused on the relatively conserved N gene of SARS-CoV-2. We rearranged and ubiquitin-modified the N gene to effectively disrupt its function, promote antigen proteolysis, reduce the production of N protein-specific

antibodies, and achieve efficient presentation of $CD8^+$ T lymphocyte epitopes, inducing a strong cellular immune response. Additionally, following previous studies, we mutated ubiquitination sites by replacing the G76 residue at the isopeptidase site with non-cleavable valine residues (UbVR and UbVV), enhancing the stability of the ubiquitin-protein complex. To ensure efficient transcription, a Kozak sequence was placed upstream of the Ub/WT-N (Ub/RE-N) combination sequence. The SARS-CoV-2 WT-N and Re-N mRNA vaccines constructed in this study were validated in animal models for their protective efficacy. The results indicated that the $CD8^+$ T lymphocyte-mediated protective cellular immune response could effectively reduce the risk of cytokine storm formation, decrease tissue cell apoptosis and vascular damage, and counteract the pathogenic mechanisms associated with viral infections. In summary, the combination of disrupting N protein function and enhancing $CD8^+$ T cell epitope presentation through ubiquitination modifications demonstrated a promising strategy in mRNA vaccine design. This approach not only elicited robust cellular immunity but also provided a broad spectrum of protection against various SARS-CoV-2 variants, highlighting the potential for developing effective vaccines against rapidly mutating viruses.

Neutralizing antibodies prevent viral entry, but the body also requires SARS-CoV-2-specific $CD4^+$ T helper cells to induce these specific antibodies [39]. Similarly, $CD8^+$ cytotoxic T cells are crucial for recognizing and killing infected cells, especially in the lungs during infection [40]. Therefore, T cell epitopes are key to understanding immune pathogenesis and validating vaccines and therapies, but these remain unknown in SARS-CoV-2-infected mice [41, 42]. Based on previous studies, we identified SARS-CoV-2-specific T cell epitopes recognized by $CD4^+$ and $CD8^+$ T cells in C57BL/6 mice. We incorporated ubiquitin modifications to construct a COVID-19 epitope mRNA vaccine. Vaccination with the COVID-19 epitope mRNA vaccine induced virus-specific T cells that led to faster viral clearance and reduced pathological changes in the lungs of SARS-CoV-2-infected mice, as well as lower viral RNA loads. This indicates that SARS-CoV-2-specific $CD4^+$ and $CD8^+$ T cells can protect mice from SARS-CoV-2 infection even in the absence of neutralizing antibodies. This suggests that generating an effective virus-specific cellular response is critical for coronavirus clearance [40].

In our study of novel SARS-CoV-2 mRNA vaccine candidates, we observed that the cross-protective properties of the six designed vaccines might be attributed to their diversified antigen presentation, which activates the immune system. By considering the antigenic characteristics of different viral strains in vaccine design, our vaccines elicited broad immune responses, providing effective cross-variant protection. Among these, the RBD-Fe, RE-N, and COVID-19 epitope vaccines demonstrated the most effective performance. This finding is significant for vaccine development and application in the face of the constantly mutating SARS-CoV-2, offering robust support for future efforts to address viral mutation challenges.

Author contributions

M.-Y.T. designed the experiments. J.-H.X. wrote the paper. T.Y. performed the majority of the experiments and analyzed the data. X.-Y.Z. drafted the original paper.

Funding

This work was supported by the Changchun Science and Technology Development Plan Project (21ZGY30).

Data availability

No datasets were generated or analysed during the current study.

Declarations

Ethics approval and consent to participate

All animal experiments in this study were approved by the Institutional Animal Care and Use Committee (IACUC) of the Institute of Medical Experimental Animals, Chinese Academy of Medical Sciences, with approval number IACUC of AMMS-11-2022-032.

Consent for publication

Not applicable.

Competing interests

The authors declare no competing interests.

Received: 12 January 2025 / Accepted: 10 May 2025
Published online: 24 May 2025

References

1. Silvio S, Annika K, Tuba BG, Reto L, Etori MAM, Lisa T, Jenna K, Volker NT. SARS-CoV-2 biology and host interactions. Nat Rev Microbiol 22(4) (2024).
2. Zhu N, Zhang D, Wang W, Li X, Yang B, Song J, Zhao X, Huang B, Shi W, Lu R, Niu P, Zhan F, Ma X, Wang D, Xu W, Wu G, Gao GF, Tan W. A novel coronavirus from patients with pneumonia in China, 2019. N Engl J Med. 2020;382(8):727–33.
3. Guan WJ, Ni ZY, Hu Y, Liang WH, Ou CQ, He JX, Liu L, Shan H, Lei CL, Hui DSC, Du B, Li LJ, Zeng G, Yuen KY, Chen RC, Tang CL, Wang T, Chen PY, Xiang J, Li SY, Wang JL, Liang ZJ, Peng YX, Wei L, Liu Y, Hu YH, Peng P, Wang JM, Liu JY, Chen Z, Li G, Zheng ZJ, Qiu SQ, Luo J, Ye CJ, Zhu SY, Zhong NS. Clinical characteristics of coronavirus disease 2019 in China. N Engl J Med. 2020;382(18):1708–20.
4. Alexandra W, Young-Jun CP, Alejandra TM, Abigail W, Andrew M, David TV. Structure, function, and antigenicity of the SARS-CoV-2 Spike glycoprotein. Cell 181(2) (2020).
5. Kim D, Lee JY, Yang JS, Kim JW, Kim VN, Chang H. The architecture of SARS-CoV-2 transcriptome. Cell. 2020;181(4):914–e92110.
6. Dong E, Du H, Gardner L. An interactive web-based dashboard to track COVID-19 in real time. Lancet Infect Dis. 2020;20(5):533–4.
7. Chuang L, Jie Y, Rahma I, Lili W, Mingzhe N, Shengxia Y, Jie L, Chao W, Yuxin C. CoronaVac-induced antibodies that facilitate Fc-mediated neutrophil phagocytosis track with COVID-19 disease resolution. Emerg Microbes Infect (0) (2024).
8. Jae-Hun A, Jisun L, Gahyun R, Na-Young L, Hee-Jin B, Euna K, Kang-Min H, Ji-Eun K, Hyo-Jung P, Soyeon Y, Sung Pil K, Eun-Kyoung B, Gyochang K, Jae-Hwan N. K. Byeong-Cheol, impact of administration routes and dose frequency on the toxicology of SARS-CoV-2 mRNA vaccines in mice model. Arch Toxicol (0) (2024).

9. Sahin U, Karikó K, Türeci Ö. mRNA-based therapeutics–developing a new class of drugs. Nat Rev Drug Discov. 2014;13(10):759–80.
10. Pardi N, Hogan MJ, Porter FW, Weissman D. mRNA vaccines - a new era in vaccinology. Nat Rev Drug Discov. 2018;17(4):261–79.
11. Vogel AB, Lambert L, Kinnear E, Busse D, Erbar S, Reuter KC, Wicke L, Perkovic M, Beissert T, Haas H, Reece ST, Sahin U, Tregoning JS. Self-Amplifying RNA vaccines give equivalent protection against influenza to mRNA vaccines but at much lower doses. Mol Ther. 2018;26(2):446–55.
12. Xie C, Yao R, Xia X. The advances of adjuvants in mRNA vaccines. NPJ Vaccines. 2023;8(1):162.
13. Gao Q, Bao L, Mao H, Wang L, Xu K, Yang M, Li Y, Zhu L, Wang N, Lv Z, Gao H, Ge X, Kan B, Hu Y, Liu J, Cai F, Jiang D, Yin Y, Qin C, Li J, Gong X, Lou X, Shi W, Wu D, Zhang H, Zhu L, Deng W, Li Y, Lu J, Li C, Wang X, Yin W, Zhang Y, Qin C. Development of an inactivated vaccine candidate for SARS-CoV-2. Science. 2020;369(6499):77–81.
14. Dai L, Gao GF. Viral targets for vaccines against COVID-19. Nat Rev Immunol. 2021;21(2):73–82.
15. Kowalski PS, Rudra A, Miao L, Anderson DG. Delivering the messenger: advances in technologies for therapeutic mRNA delivery. Mol Ther. 2019;27(4):710–28.
16. Hassett KJ, Benenato KE, Jacquinet E, Lee A, Woods A, Yuzhakov O, Himansu S, Deterling J, Geilich BM, Ketova T, Mihai C, Lynn A, McFadyen I, Moore MJ, Senn JJ, Stanton MG, Almarsson Ö, Ciaramella G, Brito LA. Optimization of lipid nanoparticles for intramuscular administration of mRNA vaccines. Mol Ther Nucleic Acids. 2019;15:1–11.
17. Yu T, Zhang C, Xing J, Zhang T, Xu Z, Di Y, Yang S, Jiang R, Tang J, Zhuang X, Jin N, Tian M. Ferritin-binding and ubiquitination-modified mRNA vaccines induce potent immune responses and protective efficacy against SARS-CoV-2. Int Immunopharmacol. 2024;129:111630.
18. Zeli Z, Jose M, Camila C, Jennifer HD, Carolyn Rydyznski MM, Rosa Isela G, Fernanda C, Alba HG, Alison T, James C, Alexandar EE, Christina K, Benjamin G, Nathaniel B, April IF, Daniela W, Alessandro S, Shane C. Humoral and cellular immune memory to four COVID-19 vaccines. Cell 185(14) (2022).
19. Sahin U, Muik A, Derhovanessian E, Vogler I, Kranz LM, Vormehr M, Baum A, Pascal K, Quandt J, Maurus D, Brachtendorf S, Lörks V, Sikorski J, Hilker R, Becker D, Eller AK, Grützner J, Boesler C, Rosenbaum C, Kühnle MC, Luxemburger U, Kemmer-Brück A, Langer D, Bexon M, Bolte S, Karikó K, Palanche T, Fischer B, Schultz A, Shi PY, Fontes-Garfias C, Perez JL, Swanson KA, Loschko J, Scully IL, Cutler M, Kalina W, Kyratsous CA, Cooper D, Dormitzer PR, Jansen KU, Türeci Ö. COVID-19 vaccine BNT162b1 elicits human antibody and T(H)1 T cell responses. Nature. 2020;586(7830):594–9.
20. Anderson EJ, Rouphael NG, Widge AT, Jackson LA, Roberts PC, Makhene M, Chappell JD, Denison MR, Stevens LJ, Pruijssers AJ, McDermott AB, Flach B, Lin BC, Doria-Rose NA, O'Dell S, Schmidt SD, Corbett KS, Swanson PA 2nd, Padilla M, Neuzil KM, Bennett H, Leav B, Makowski M, Albert J, Cross K, Edara VV, Floyd K, Suthar MS, Martinez DR, Baric R, Buchanan W, Luke CJ, Phadke VK, Rostad CA, Ledgerwood JE, Graham BS. Beigel, safety and immunogenicity of SARS-CoV-2 mRNA-1273 vaccine in older adults. N Engl J Med. 2020;383(25):2427–38.
21. Thompson MG, Burgess JL, Naleway AL, Tyner HL, Yoon SK, Meece J, Olsho LEW, Caban-Martinez AJ, Fowlkes A, Lutrick K, Kuntz JL, Dunnigan K, Odean MJ, Hegmann KT, Stefanski E, Edwards LJ, Schaefer-Solle N, Grant L, Ellingson K, Groom HC, Zunie T, Thiese MS, Ivacic L, Wesley MG, Lamberte JM, Sun X, Smith ME, Phillips AL, Groover KD, Yoo YM, Gerald J, Brown RT, Herring MK, Joseph G, Beitel S, Morrill TC, Mak J, Rivers P, Harris KM, Hunt DR, Arvay ML, Kutty P, Fry AM, Gaglani M. Interim estimates of vaccine effectiveness of BNT162b2 and mRNA-1273 COVID-19 vaccines in preventing SARS-CoV-2 infection among health care personnel, first responders, and other essential and frontline Workers -. Volume 70. Eight U.S. Locations,; 2021. pp. 495–500. December 2020-March 2021, MMWR Morb Mortal Wkly Rep. 13.
22. Dagan N, Barda N, Kepten E, Miron O, Perchik S, Katz MA, Hernán MA, Lipsitch M, Reis B, Balicer RD. BNT162b2 mRNA Covid-19 vaccine in a nationwide mass vaccination setting. N Engl J Med. 2021;384(15):1412–23.
23. Frank G Jr, Wanbo T, Denis V, Yi Z, Xiujuan Z, Juan S, Xinyi W, Ning W, Lanying D, Liang Q. A vaccine inducing solely cytotoxic T lymphocytes fully prevents Zika virus infection and fetal damage. Cell Rep 35(6) (2021).
24. Laury N, Florence P, Marwa EH, Léa D, Craig F, Sylvain C, Aurélie W, Giuseppe P, Sandra Z, Mireille C, Gerard Z, Yves L, Véronique G. Subunit protein CD40. SARS.CoV2 vaccine induces SARS-CoV-2-specific stem cell-like memory CD8(+) T cells. EBioMedicine 111(0) (2024).
25. Shambhunath C, Isis K, Soner Y, Rani S, Kena A SS, Tania F, Raveen R, Raquel M-M, Sonia J, Olga G, Philip M, Timothy C, Jessie Q, Thomas L, Jillian AJ, Cassandra GT, Justin A, Kristin DT, Arthur I, Paula C, Tara C, Philip D, Edward RD, Vinay J Jr, Shannan H-U, Journey C, Deepak K, Jane F, Carles AM-R, Meagan M, Florian K, Michael S, Adolfo G-S. Modeling SARS-CoV-2: comparative pathology in Rhesus macaque and golden Syrian Hamster models. Toxicol Pathol 50(3) (2022).
26. Ashutosh S, Rahul Soloman S, Phulen S, Gitika B, Rupa J, Hardeep K, Amit Raj S, Ajay P, Bikash M. A comprehensive review of animal models for coronaviruses: SARS-CoV-2, SARS-CoV, and MERS-CoV. Virol Sin 35(3) (2020).
27. Peter H, Shun JI, Kiyoko I-H, Tadashi M, Maki K, Suzanne S, Tamarand MD, Astha LJ, Samantha L, Gagandeep S, Stephanie F, Baoling LY, James Brett C, Zhenlu C, Bradley W, Juan M, Katharine F, Michiko U, Noriko N, Mutsumi I, Ryan W, Ryuta U, Prajakta W, Matthew G, Rong L, Yuko S-T, Yanan L, Deanna L, Jorge O, Juan EH-O, Amy PH, Karl RC, Kelsey F, Mit RP, Abby O, Lok-Yin W, Roy B, Allen C, Zhongde W, Venkata-Viswanadh E, Zhenlu C, John F, Trushar J, Thomas F, Jennifer D, Lisa K, Patrick S, Ana Silvia G-R, Emilia Mia S, Lauren C, Harm AvB, Viviana S, Daniel D, Nancy CS, Larissa JT, Hiroshi BU, Seiya Y, Masaki I, Stanley P, Richard W, Robert JS, Mehul A, Adolfo SG-S, Michael S, Tadaki S, Adrianus B. C M, D. Michael S, K. Yoshihiro, SARS-CoV-2 Omicron virus causes attenuated disease in mice and hamsters, Nature 603(7902) (2022).
28. Sin Fun S, Li-Meng Y, Alex C, Kevin WHF, Ka-Tim C, Alvina W, Prathanporn YLK, Ranawaka P, M AP, Leo P, John LMN, Malik MP. Y. Hui-Ling, pathogenesis and transmission of SARS-CoV-2 in golden hamsters. Nature 583(7818) (2020).
29. Zhuang X, Chen L, Yang S, Xia S, Xu Z, Zhang T, Zeng B, Yu T, Yu N, Wang W, Lu H, Tian M, Jin N. R848 adjuvant laden with Self-Assembled Nanoparticle-Based mRNA vaccine elicits protective immunity against H5N1 in mice. Front Immunol. 2022;13:836274.
30. Walls A, Park Y, Tortorici M, Wall A, McGuire A, Veesler D. Structure, function, and antigenicity of the SARS-CoV-2 Spike glycoprotein. Cell. 2020;181(2):281–e2926.
31. Rebecca U, Saskia B, Verena K, Stefanie M, Franziska H, Amina A-O, Candida G, Sophie S, Christina B, Sören B, Barbara LG, Urban CS, Leonardo M, Marek W, Tina S, Martina S. SARS-CoV-2-specific cellular and humoral immunity after bivalent BA.4/5 COVID-19-vaccination in previously infected and non-infected individuals. Nat Commun 15(1) (2024).
32. Martin Š, Luděk B, Lenka P, Ondřej M, Tomáš P, Jiří J, Jakub W, Tamara B, Jan T. Protection by vaccines and previous infection against the Omicron variant of severe acute respiratory syndrome coronavirus 2. J Infect Dis 226(8) (2022).
33. Alexander U, Christina PS, Kivin J, Alekxander B, Carlota F-A, Lotte M, Dilek SI, Signe Lysemose V, Jose C, Mette ASP, Ulrik F, Santseharay R, Liselotte B, Nina W, Jens B. Neutralizing antibody and CD8(+) T cell responses following BA.4/5 bivalent COVID-19 booster vaccination in adults with and without prior exposure to SARS-CoV-2. Front Immunol 15(0) (2024).
34. Milja B, Arttu R, Pekka K, Jemna H, Sari M, Eda A, Pamela Ö, Larissa L, Olli R, Arja P, Rauno N, Alina AI, Alex-Mikael B, Qiushui H, Johanna L, Paula T, Lauri AI, Pinja J, Ilkka J, Laura K. Long-term COVID-19 vaccine- and Omicron infection-induced humoral and cell-mediated immunity. Front Immunol 15(0) (2024).
35. Altmann DM, Boyton RJ. SARS-CoV-2 T cell immunity: specificity, function, durability, and role in protection. Sci Immunol 5(49) (2020).
36. Sette A, Crotty S. Adaptive immunity to SARS-CoV-2 and COVID-19. Cell. 2021;184(4):861–80.
37. Grifoni A, Weiskopf D, Ramirez SI, Mateus J, Dan JM, Moderbacher CR, Rawlings SA, Sutherland A, Premkumar L, Jadi RS, Marrama D, de Silva AM, Frazier A, Carlin AF, Greenbaum JA, Peters B, Krammer F, Smith DM, Crotty S, Sette A. Targets of T cell responses to SARS-CoV-2 coronavirus in humans with COVID-19 disease and unexposed individuals. Cell. 2020;181(7):1489–e150115.
38. Yewdell JW, Bennink JR. Mechanisms of viral interference with MHC class I antigen processing and presentation. Annu Rev Cell Dev Biol. 1999;15:579–606.
39. Ahmed R, Gray D. Immunological memory and protective immunity: Understanding their relation. Science. 1996;272(5258):54–60.
40. Wanbo T, Shengyong F, Benjie C, Shuaiyao L, Guangyu Z, Dong C, Wenhai Y, Liting R, Huicheng S, Jing L, Zhuming C, Mujia P, Xu T, Penghua W, Jinzhong L, Qiangming S, Xiaozhong P, Gong C. An mRNA-based T-cell-inducing antigen strengthens COVID-19 vaccine against SARS-CoV-2 variants. Nat Commun 14(1) (2023).
41. Tarke A, Sidney J, Methot N, Yu ED, Zhang Y, Dan JM, Goodwin B, Rubiro P, Sutherland A, Wang E, Frazier A, Ramirez SI, Rawlings SA, Smith DM, da Silva Antunes R, Peters B, Scheuermann RH, Weiskopf D, Crotty S, Grifoni A, Sette A. Impact of SARS-CoV-2 variants on the total CD4(+) and CD8(+) T cell reactivity in infected or vaccinated individuals. Cell Rep Med. 2021;2(7):100355.
42. Peng Y, Mentzer AJ, Liu G, Yao X, Yin Z, Dong D, Dejnirattisai W, Rostron T, Supasa P, Liu C, López-Camacho C, Slon-Campos J, Zhao Y, Stuart DI, Paesen

GC, Grimes JM, Antson AA, Bayfield OW, Hawkins D, Ker DS, Wang B, Turtle L, Subramaniam K, Thomson P, Zhang P, Dold C, Ratcliff J, Simmonds P, de Silva T, Sopp P, Wellington D, Rajapaksa U, Chen YL, Salio M, Napolitani G, Paes W, Borrow P, Kessler BM, Fry JW, Schwabe NF, Semple MG, Baillie JK, Moore SC, Openshaw PJM, Ansari MA, Dunachie S, Barnes E, Frater J, Kerr G, Goulder P, Lockett T, Levin R, Zhang Y, Jing R, Ho LP, Cornall RJ, Conlon CP, Klenerman P, Screaton GR, Mongkolsapaya J, McMichael A, Knight JC, Ogg G, Dong T. Broad and strong memory CD4(+) and CD8(+) T cells induced by SARS-CoV-2 in UK convalescent individuals following COVID-19. Nat Immunol. 2020;21(11):1336–45.

Publisher's note